(*20*). A yeast gene capable of encoding a 120-kD putative RNA helicase protein rescued the mutant phenotype of a conditional yeast mutant defective in export of polyadenylate RNA (*21*). Given the RNA-binding and shuttling ability of helicase A, it is conceivable that it participates in certain cellular RNA export pathways. Simian retroviruses have likely tapped into this pathway and use helicase A as a cofactor in nuclear export of CTE-containing RNA by means of a specific RNA-protein interaction. It will be interesting to determine whether helicase A also plays a role in the replication cycle of other retroviruses, including complex retroviruses such as HIV.

REFERENCES AND NOTES

1. M. Bray *et al*., *Proc. Natl. Acad. Sci. U.S.A.* **91**, 1256 (1994).
2. A. S. Zolotukhin, A. Valentin, G. N. Pavlakis, B. K. Felber, *J. Virol.* **68**, 7944 (1994).
3. J. M. Yeakley, J. P. Morfin, M. G. Rosenfeld, X. D. Fu, *Proc. Natl. Acad. Sci. U.S.A.* **15**, 7582 (1996).
4. H. Tang, Y. Xu, F. Wong-Staal, *Virology* **228**, 333 (1997).
5. Y. Xu, W. H. Fischer, T. R. Reddy, F. Wong-Staal, *J. Biomed. Sci.* **3**, 82 (1996).
6. Sequences of three microsequenced peptides are as follows: peptide 1, AENN(C)EVGA(C)GYGGVXG (matching amino acids 121 to 136 of helicase A); peptide 2, YTQVGPDHNR (matching amino acids 200 to 209 of helicase A); peptide 3, LAQFEPSQRF (matching amino acids 315 to 323 of helicase A) (*22*); C. Lee and J. Hurwitz, *J. Biol. Chem.* **268**, 16822 (1993).
7. C. Lee and J. Hurwitz, *J. Biol. Chem.* **267**, 4398 (1992).
8. B. E. Meyer and M. H. Malim, *Genes Dev.* **8**, 1538 (1994).
9. U. Fischer, J. Huber, W. C. Boelens, I. W. Mattaj, R. Luhrmann, *Cell* **82**, 475 (1995).
10. L. Luznik, *et al*., *AIDS Res. Hum. Retroviruses* **11**, 795 (1993).
11. H. Tang and F. Wong-Staal, unpublished data.
12. H. Tang, G. M. Gaietta, W. H. Fischer, M. H. Ellisman, F. Wong-Staal, data not shown.
13. The sense and antisense RNA probes were prepared by in vitro transcription, with 2′-deoxyuridine-5′-triphosphate coupled to digoxigenin (digoxigenin-11-dUTP) (Boehringer Mannheim) as a label. HeLa cells were attached to glass cover slips (Fisher) coated with poly-D-lysine (Sigma). Sixteen, 20, and 26 hours after the addition of DNA-calcium precipitate, cells were washed in phosphate-buffered saline (PBS) until no precipitate was visible and then fixed with 4% paraformaldehyde for 30 min. The following steps were performed to facilitate accessibility of CTE and to reduce nonspecific binding of the RNA probe: 2 min in 0.5% Triton X-100 (in PBS), 5 min in 0.5 N HCl, 10 min in acetylation buffer (583 μl of triethanolamine and 125 μl of acetic anhydride in 50 ml of diethyl pyrocarbonate–treated water). Each step was followed by two brief washes in PBS, and then 30 μl of prehybridization solution [containing 50% formamide, 5× standard saline citrate (SSC), 5× Denhardt's reagent, single-stranded DNA (50 μg/ml), tRNA (25 μg/ml)] lacking the probe was applied to each sample. Samples were prehybridized at 42°C for 1 hour in a humid chamber. At the end of the prehybridization step, samples were rinsed in 5× SSC and prepared for the hybridization step: 30 μl of prehybridization solution, containing a 1:100 dilution of the digoxigenin-labeled RNA probes (previously denatured at 65°C for 10 min) was applied to each cover slip, covered with a glass coverslip, and sealed with rubber cement. Hybridization was carried out overnight at 42°C in a humid chamber. The posthybridization washes were performed in SSC wash buffer at high stringency (2× to 0.1×). Samples were treated with ribonuclease to remove RNA probes that did not hybridize to the target RNA. Detection of the hybridized RNA probes was performed with an antibody to digoxigenin F(ab) coupled to alkaline phosphatase (Boehringer Mannheim) followed by a colorimetric reaction with nitroblue tetrazolium and 5-bromo-4-chloro-3-indolyl phosphate, or by hybridization with a biotinylated secondary antibody and detection with streptavidin Cy5 conjugate. The protein was detected with a rabbit polyclonal antibody to human helicase A. The polyclonal antibody was then immunodetected with a donkey antibody to rabbit immunoglobulin G coupled to Cy5 (detection of RNA probe with alkaline phosphatase) or to fluorescein isothiocyanate (FITC) (RNA indirectly labeled with Cy5). The samples were viewed with a Bio-Rad MRC 1024 laser-scanning confocal system coupled to a Zeiss Axiovert 35M microscope with a planapochromatic objective (×40, 1.3 numerical aperture, oil immersion).
14. S. Píñol-Roma and G. Dreyfuss, *Nature* **355**, 730 (1992).
15. F. B. Sehgal, J. E. Darnell, I. Tamm, *Cell* **9**, 473 (1976).
16. R. P. Perry and D. E. Kelly, *J. Cell. Physiol.* **76**, 127 (1970).
17. H. Tang and F. Wong-Staal, unpublished data.
18. C. Tabernero, A. S. Zolotukhin, A. Valentin, G. N. Pavlakis, B. K. Felber, *J. Virol.* **70**, 5998 (1996).
19. R. K. Ernst, M. Bray, D. Rekosh, M. Hammarskjöd, *Mol. Cell. Biol.* **17**, 135 (1997).
20. M. Ohno and Y. Shimura, *Genes Dev.* **10**, 997 (1996).
21. S. Liang, M. Hitomi, Y. Hu, Y. Liu, A. M. Tartakoff, *Mol. Cell. Biol.* **16**, 5139 (1996).
22. Abbreviations for the amino acid residues are: A, Ala; C, Cys; D, Asp; E, Glu; F, Phe; G, Gly; H, His; I, Ile; K, Lys; L, Leu; M, Met; N, Asn; P, Pro; Q, Gln; R, Arg; S, Ser; T, Thr; V, Val; W, Trp; and Y, Tyr.
23. Large amounts of biotinylated RNA were made with the Megashortscript in vitro transcription kit (Ambion) in the presence of biotin-21-UTP (Clontech). Nuclear extract (200 μl) was incubated with about 100 μg of biotinylated CTE wild-type or mutant RNA at 4°C overnight before being subjected to affinity purification with streptavidin-conjugated agarose beads (BRL). Proteins that were trapped in beads were eluted by eating in SDS-PAGE buffer at 65°C for 5 min and then run on a 6% polyacrylamide gel. Proteins were either visualized by Coomassie blue staining, transhlp; &.5qhferred onto a PVDF membrane and stained with 0.1% amido black 10B, or detected by antibodies. For protein internal sequence determination, the protein band was excised from the PVDF membrane and subjected to trypsin digestion, peptides were purified by high-performance liquid chromatography, and three well-separated fractions were selected for microsequencing. RNA used in gel-shift assays was labeled with [^{32}P]UTP and purified from polyacrylamide gel. Purified human helicase A (100 to 200 ng) was then incubated with RNA probe (1×10^5 cpm) for 15 min at room temperature. The reaction mixture was then mixed with RNA loading buffer (10% glycerol, 0.01% bromophenol blue, 0.01% xylene cyanol) and run on a 4% polyacrylamide gel (acrylamide:bisacrylamide = 60:1). The gel was subsequently dried and subjected to autoradiography.
24. HeLa cells were grown in slide chambers. Transfections were done by conventional calcium phosphate precipitation and cells were fixed for immunostaining 26 to 28 hours after transfection. Cells were fixed in methanol and acetone (1:1) for 2 min, washed extensively with PBS, and blocked with 3% bovine serum albumin in PBS for 10 min before the first antibodies were applied. The polyclonal antibody against helicase A was provided by Lee and Hurwitz (*6*). FITC-coupled goat antibody to rabbit immunoglobulin G was used as a second antibody to detect helicase A. Cells grown on coated glass cover slips, fixed with 4% paraformaldehyde, and permeabilized by 0.5% Triton X-100 gave essentially the same results for protein staining.

25. We are indebted to C. Lee and J. Hurwitz for purified helicase A protein and a polyclonal antibody against human helicase A. R. Moy helped with the constructions of pDMCTE and pDCTE. M. Park performed the protein sequence analysis. Supported in part by grants NIH RR 04050 and NS 14718 (M.H.E.) and by the University of California, San Diego, Center for AIDS Research (F.W-S).

16 January 1997; accepted 4 April 1997

Induction of Leaf Primordia by the Cell Wall Protein Expansin

Andrew J. Fleming,* Simon McQueen-Mason, Therese Mandel, Cris Kuhlemeier†

Expansins are extracellular proteins that increase plant cell wall extensibility in vitro. Beads loaded with purified expansin induced bulging on the leaf-generating organ, the apical meristem, of tomato plants. Some of these bulges underwent morphogenesis to produce leaflike structures, resulting in a reversal of the direction of phyllotaxis. Thus, expansin can induce tissue expansion in vivo, and localized control of tissue expansion may be sufficient to induce leaf formation. These results suggest a role for biophysical forces in the regulation of plant development.

Leaves form by reiterative organogenesis from a specialized organ, the shoot apical meristem (*1*). Although spatial domains of transcription factor activity can dictate where and when a leaf is initiated, the mechanism by which this information is transduced into morphogenesis is unknown (*2*). One model predicts that the regulation of epidermal cell wall extensibility controls tissue expansion and thus the initial steps of primordium formation (*3*). Recently, a family of cell wall proteins, expansins, that modulate cell wall extension in vitro has been characterized, although the ability of these proteins to induce cell expansion in vivo was not demonstrated (*4*). We now show that the localized application of expansin to the apical meristem induces expansion in living tissue and that the resultant bulging is sufficient to induce primordium formation.

In the tomato plant, leaves are initiated

in a spiral in which the youngest primordium is designated P1, the next oldest P2, and so on in a developmental gradient (Fig. 1, A and B). The position of the cells from which the next leaf primordia (I1 and I2) arise can be predicted. Biophysical analysis suggests that the outermost cell layers of the apical meristem are under tension, whereas the inner cell mass is subjected to compression (3), in which case a localized increase in cell wall extensibility in the outer cells of the meristem should result in expansion and accompanying bulging out of the tissue (3). To test this hypothesis, we placed beads loaded with purified expansin onto the I2 position (5) and indeed observed the formation of a bulge (I′2) at the position of the bead during the subsequent plastochron (Fig. 1, C and D). At the same time, the formation of a primordium at position I1 was suppressed.

In a first series of experiments, 37 of the 122 apices analyzed showed some effect 5 days after treatment, with a broad spectrum of changes observed (Table 1). Confocal laser-scanning microscopy (6) indicated that several of the expansin-induced bulges were incomplete, with internal areas devoid of tissue surrounded by an intact surface layer (Fig. 1E). Most of the component cells of these bulges were not substantially enlarged, suggesting that expansin-induced tissue expansion was accompanied by cell division. In seven apices, intact primordia were observed at the I2 position where the expansin-loaded beads had been positioned.

In a second series of experiments, in which the apices were analyzed 14 days after expansin treatment, 9 of the 70 apices examined generated leaflike organs at the I2 position (Fig. 2A and Table 1). These organs were green, produced trichomes, and had intact internal tissue (Fig. 2B). However, cytological differentiation was aberrant, with no vascular differentiation apparent. Nevertheless, in situ hybridization (7) revealed the expression of an *rbc*S gene previously shown to be a positive marker for leaf differentiation and a negative marker for the apical meristem (8) (Fig. 2C). Some of the expansin-induced primordia were more elongated (Fig. 2D) and, in addition to lacking appropriate cellular differentiation (Fig. 2E), did not express the *rbc*S marker gene (Fig. 2F).

Analysis of apices in which beads loaded with various substances (boiled expansin, buffer, bovine serum albumin, cellulase, and oligogalacturonic acid) were placed at the I2 position did not reveal any induction of primordia, indicating that the effects observed with the expansin-loaded beads were specific (Table 1).

The generation of a primordium at the I2 position after expansin treatment resulted in a reversal of the subsequent phyllotaxis of the plant. The formation of a structure (I′2) at position I2 suppressed the initiation of the primordium at position I1 (Fig. 3, A and B). Thus, the anticlockwise order of leaf initiation from P4 to P1 became reversed to clockwise for P1 to I′2 (Fig. 3, C and D). This reversal of phyllo-

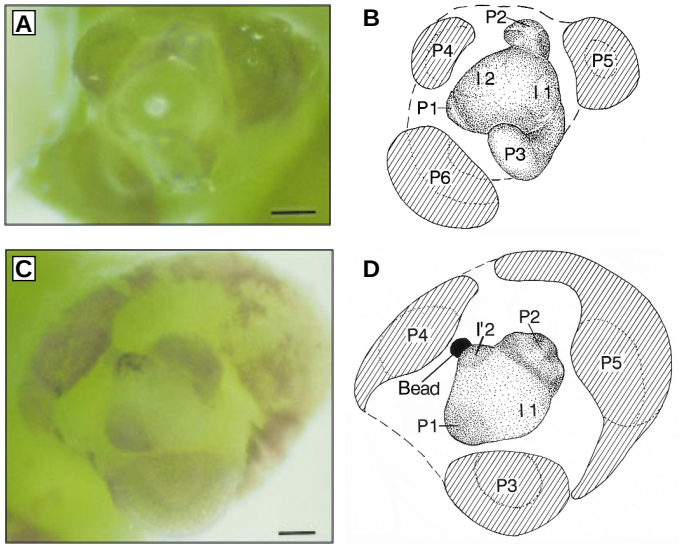

Fig. 1. Induction of primordia by expansin. (**A**) Tomato apex showing phyllotaxis. (**B**) Diagram of apex in (A). The meristem has generated primordia P6 to P1. The next leaves will arise at position I1 and then I2. (**C**) Apex of a plant 5 days after the placing of expansin-loaded beads (*5*) at I2. (**D**) Diagram of apex in (C). A bulge, I′2, on the apical meristem is present adjacent to an expansin-loaded bead. (**E**) Confocal laser-scanning microscopy section (*6*) through an incomplete bulge at the I2 position induced by expansin. Samples (A) and (C) were stained with safranin red to reveal cut surfaces, shown as hatched areas in (B) and (D). Scale bars: 50 μm (A and C) and 20 μm (E).

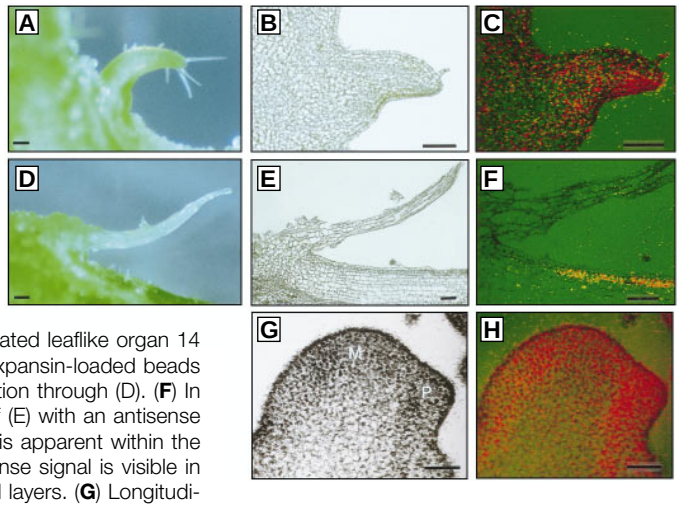

Fig. 2. Induction of leaflike structures by expansin. (**A**) An intact leaflike organ 14 days after positioning of expansin-loaded beads on the I2 position. (**B**) Section (*7*) through (A). (**C**) In situ hybridization (*7*) of (B) with an antisense probe for the leaf marker gene *rbcS*. Signals (red dots) are apparent throughout the structure. (**D**) An elongated leaflike organ 14 days after positioning of expansin-loaded beads on the I2 position. (**E**) Section through (D). (**F**) In situ hybridization of part of (E) with an antisense probe for *rbcS*. No signal is apparent within the structure, although an intense signal is visible in the subepidermal stem cell layers. (**G**) Longitudinal section through a vegetative apex showing the meristem (M) and primordium (P). (**H**) In situ hybridization of (G) with an antisense probe for expansin (*15*). A relatively high signal is apparent in the emerging leaf primordium. Scale bars: 200 μm (A through F) and 25 μm (G and H).

A. J. Fleming, T. Mandel, C. Kuhlemeier, Institute of Plant Physiology, University of Bern, Altenbergrain 21, CH-3013 Bern, Switzerland.
S. McQueen-Mason, Department of Biology, The Plant Laboratory, University of York, York YO1 5YW, UK.

*Present address: Institute of Plant Sciences, Eidgenössische Technische Hochschule–Zürich, CH-8092 Zürich, Switzerland.
†To whom correspondence should be addressed. E-mail: kuhlemeier@pfp.unibe.ch

taxis was maintained during subsequent generation of leaf primordia by the meristem (Fig. 3, E and F). Thus, the formation of leaf primordia around the meristem after the formation of an I′2 structure appeared to follow the classical rules by which the site of leaf primordium initiation is influenced by the adjacent preexisting leaf primordia (*9*). In this context, the I′2 structures functioned as leaves.

We suggest that, in our experiments, expansin induces changes in the cell wall that lead to an altered physical stress pattern in the meristem, so that tissue bulging occurs and, as a result, cells gain "primordium" identity (*2*, *3*). The observed frequency of incomplete leaf structures is consistent both with a requirement for endogenous factors in the correct completion of leaf development (*10*) and with a spatiotemporal specificity of expansin action. A role for endogenous expansin in leaf initiation is indicated by in situ hybridization analysis showing not only that expansin genes are expressed in the apical meristem, but also that transcript abundance is highest in cells forming a primordium bulge (Fig. 2, G and H).

Our data add to a growing body of evidence that the physical environment influences morphogenesis and differentiation (*3*, *11*), that signaling events (of either a chemical or physical nature) occur within the meristem (*1*, *3*), and that cell-wall components are determinantal for development (*12*). Although, in a few instances, extracellular proteins have been identified that can affect plant morphogenesis, such as arabinogalactan proteins (*13*) and cell wall enzymes (*14*), the mechanism by which these effects are transduced is unclear. We have now described specific morphogenetic effects of a defined gene product that are consistent with both the expected biochemical action of the protein (*4*) and established biophysical theories of leaf initiation (*3*). Our data suggest that cell wall structure plays a regulatory role in plant morphogenesis.

Table 1. Specific induction of leaflike structures on the apical meristem by expansin. Beads loaded with various agents in 50 mM sodium acetate buffer (pH 4.8) were manipulated onto the I2 position of meristems (*5*). After 5 or 14 days, the apices were analyzed with either a binocular microscope or confocal laser-scanning microscopy (*6*).

Agent	5 days			14 days		
	No. of apices analyzed	Altered meristem surface	Intact leaflike organs	No. of apices analyzed	Altered meristem surface	Intact leaflike organs
Expansin	122	37	7	70	11	9
Boiled expansin	37	1	0	31	0	0
Buffer alone	31	0	0	25	0	0
BSA* [2% (w/v)]	47	0	0	31	0	0
Cellulase† (50 μg/ml)	40	0‡	0	22	0	0
OGA§ (0.1 mg/ml)	32	0	0	38	0	0

*BSA, bovine serum albumin. †Cellulase was endocellulase I purified from *Trichoderma viridi*. ‡Several (18/40) cellulase-treated apices showed necrosis, but no bulges or organized structures, at the I2 position. §OGA, oligogalacturonic acid (DP 12-30) purified from tomato (*16*).

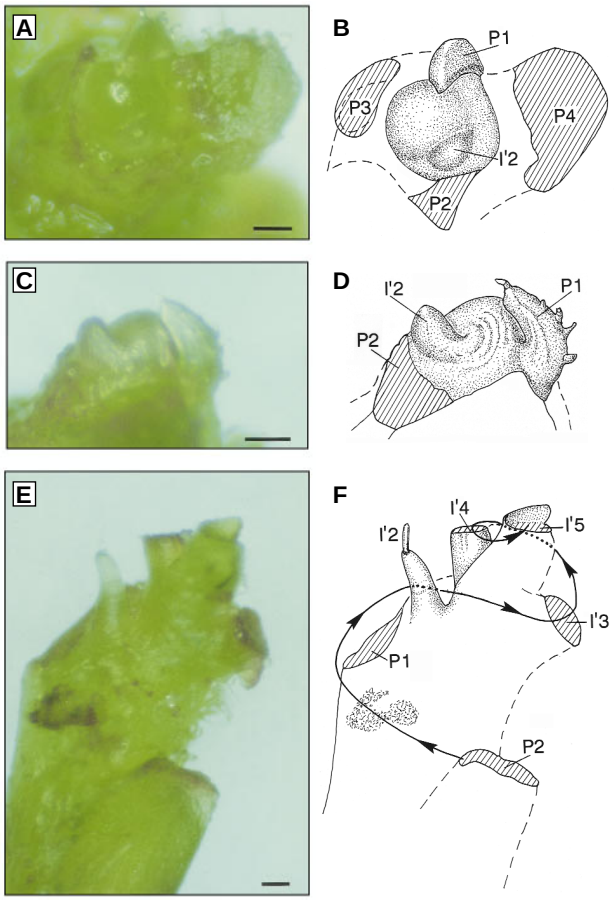

Fig. 3. Reversal of the direction of phyllotaxis by expansin-induced primordia. (**A**) Distal view of an apex that has generated an organ at the I2 position 5 days after expansin treatment. (**B**) Diagram of (A). Phyllotaxis P4 to P1 is anticlockwise. Primordium I′2 is clockwise from P1. (**C**) Side view of apex in (A). (**D**) Diagram of (C). The insertion point of the I′2 primordium lies distal and clockwise to that of P1. (**E**) View along the stem of a plant that has generated several primordia subsequent to the production of the structure at I′2. (**F**) Diagram of (E). Phyllotaxis P2 to P1 is clockwise. Twenty-one days after the induction of the I′2 leaflike structure, phyllotaxis of the subsequent leaves (I′3 to I′5) is anticlockwise. In (A), (C), and (E), primordia have been cut to reveal the meristem and the tissue stained with safranin red to reveal cut surfaces [shown as hatched areas in (B), (D), and (F)]. Scale bars: 50 μm (A and C) and 500 μm (E).

REFERENCES AND NOTES

1. T. A. Steeves and I. M. Sussex, *Patterns in Plant Development* (Cambridge Univ. Press, Cambridge, 1989); J. I. Medford, *Plant Cell* **4**, 1029 (1992); L. G. Smith and S. Hake, *ibid*., p. 1017.
2. S. Hake, *Trends Genet.* **8**, 109 (1992); D. Jackson, B. Veit, S. Hake, *Development* **120**, 405 (1994); D. Weigel and E. M. Meyerowitz, *Cell* **78**, 203 (1994).
3. J. M. L. Selker, G. L. Steucek, P. B. Green, *Dev. Biol.* **153**, 29 (1992); P. B. Green, *Ann. Bot. (London)* **77**, 515 (1996).
4. S. McQueen-Mason, D. M. Durachko, D. J. Cosgrove, *Plant Cell* **4**, 1425 (1992); S. McQueen-Mason and D. J. Cosgrove, *Proc. Natl. Acad. Sci. U.S.A.* **91**, 6574 (1994); T. Y. Shcherban *et al*., *ibid.* **92**, 9245 (1995).
5. Beads (Sephacryl HR S-300, Pharmacia) were loaded with expansin by incubation overnight at 4°C. After centrifugation and washing with 50 mM sodium acetate buffer (pH 4.8), one to five beads were positioned on the I2 position of apices with the use of a drawn capillary needle. Expansin was purified from cucumber hypocotyls (*4*) and prepared in 50 mM sodium acetate (pH 4.8). The fractions used had an extension activity of 3.5 to 4.2% per hour, with no detectable glycosidase activity. Vegetative tomato apices were dissected, leaving either P2 and P1 or only P1, intact together with a subapical region of 3 to 5 mm. Apices were cultured [G. Hussey, *J. Exp. Bot.* **22**, 688 (1971)] with a 16-hour-light, 8-hour-dark cycle at 20°C.
6. Confocal microscopy was performed as described [M. P. Running, S. E. Clark, E. M. Meyerowitz, *Methods Cell Biol.* **49**, 217 (1995)], with the exception that washing steps were shortened to retain staining of the cell wall. Apices were viewed with a Zeiss LSM 310 microscope and an argon laser, and the propidium iodide signal was visualized through an LP590 filter. Images were stored and processed with Zeiss software.
7. Tissue fixation, sectioning, and in situ hybridization with the *rbcS* and expansin probes were as described (*8*). Signals were visualized through a polarizing filter set with epifluorescent illumination, and the

silver particles were rendered red and superimposed on a bright-field image of the section. No substantial signal above background was apparent after hybridization with sense probes.
8. A. J. Fleming, T. Mandel, I. Roth, C. Kuhlemeier, *Plant Cell* **5**, 297 (1993); A. J. Fleming, T. Manzara, W. Gruissem, C. Kuhlemeier, *Plant J.* **10**, 745 (1996).
9. M. Snow and R. Snow, *Philos. Trans. R. Soc. London Ser. B* **221**, 1 (1931).
10. E. J. Szymkowiak and I. M. Sussex, *Plant Cell* **4**, 1089 (1992); S. Hantke, R. Carpenter, E. S. Coen, *Development* **121**, 27 (1995).
11. N. Wang, J. P. Butler, D. E. Ingber, *Science* **260**, 1124 (1993).
12. K. Roberts, *Curr. Opin. Cell Biol.* **6**, 688 (1994); C. Brownlee and F. Berger, *Trends Genet.* **11**, 344 (1995); R. S. Quatrano and S. L. Shaw, *Trends Plant Sci.* **2**, 15 (1997).
13. D. V. Basile, in *Bryophyte Development and Physiology*, R. N. Chopra and S. C. Bhatla, Eds. (CRC Press, Boca Raton, FL, 1990), pp. 225–243.
14. A. J. De Jong *et al*., *Plant Cell* **4**, 425 (1992).
15. An expansin clone was isolated from meristem cDNA (*8*) by reverse transcription and the polymerase chain reaction with primers designed from the published sequences (*4*). This cDNA fragment (expansin 18), which showed 73.8% identity to the cucumber sequence CuExS1 over the amplified 144 base pairs, was used as a substrate for riboprobe synthesis and in situ hybridization (*7*).
16. P. Reymond, S. Grünberger, K. Paul, M. Müller, E. E. Farmer, *Proc. Natl. Acad. Sci. U.S.A.* **92**, 4195 (1995).
17. We thank A. Buchala and E. Farmer for endocellulase and oligogalacturonic acid, respectively; I. Sussex, P. Green, C. Smart, and I. Dupuis for constructive criticism; H. Imboden for use of the confocal imaging facility; and M. Kummer for scientific artwork. Supported by a Swiss National Science Foundation grant to C.K. and A.J.F.

17 December 1996; accepted 25 March 1997

STAT3 as an Adapter to Couple Phosphatidylinositol 3-Kinase to the IFNAR1 Chain of the Type I Interferon Receptor

Lawrence M. Pfeffer,*† Jerald E. Mullersman, Susan R. Pfeffer, Aruna Murti, Wei Shi, Chuan He Yang*

STAT (signal transducers and activators of transcription) proteins undergo cytokine-dependent phosphorylation on serine and tyrosine. STAT3, a transcription factor for acute phase response genes, was found to act as an adapter molecule in signal transduction from the type I interferon receptor. STAT3 bound to a conserved sequence in the cytoplasmic tail of the IFNAR1 chain of the receptor and underwent interferon-dependent tyrosine phosphorylation. The p85 regulatory subunit of phosphatidylinositol 3-kinase, which activates a series of serine kinases, bound to phosphorylated STAT3 and subsequently underwent tyrosine phosphorylation. Thus, STAT3 acts as an adapter to couple another signaling pathway to the interferon receptor.

Interferons (IFNs) are cytokines that block the viral infection of cells, inhibit cell proliferation, and modulate cell differentiation. Type I IFNs (IFN-α, -β, and -ω) compete with each other for binding to a common cell surface receptor (IFN-R), distinct from the receptor for type II IFN (IFN-γ) (*1*). The IFN-R is composed of IFNAR1 and IFNAR2 chains (*2–4*). The IFNAR1 chain undergoes rapid ligand-dependent tyrosine phosphorylation and acts as a species-specific transducer for the actions of type I IFN, which suggests that it has a central role in signaling through the IFN-R (*5–7*). IFNs cause transduction of a signal to the nucleus that results in selective stimulation of the IFN-stimulated genes (ISGs) (*8–10*). Transcriptional activation of ISGs is mediated by the protein tyrosine kinase–dependent phosphorylation of the STAT latent cytoplasmic transcriptional activators (*11, 12*). Upon tyrosine phosphorylation, IFN-α–activated STATs (STAT1, STAT2, and STAT3) form homo- and heterodimers.

Although tyrosine phosphorylation of STATs and IFN-R are important early events in IFN signaling, serine phosphorylation events are also necessary for the induction of IFN action (*13–16*). Here, IFN-α induced the rapid tyrosine phosphorylation of the regulatory 85-kD (p85) subunit of phosphatidylinositol 3-kinase (PI 3-kinase), an upstream element in a serine kinase transduction cascade (*17, 18*). IFN-α–dependent recruitment of p85 to the IFNAR1 chain of the IFN-R required the tyrosine phosphorylation of the YSSQ and YSNE motifs that are present in the conserved IRTAM (IFN receptor tyrosine activation motif) cytosolic sequence KYSSQTSQDSGNYSNE in IFNAR1 (*19*). The IRTAM functions in the signaling through the IFN-R by specifically acting as a docking site for cytoplasmic proteins containing the Src homology 2 (SH2) domain (*6, 20*). Interaction of p85 with IFNAR1 required STAT3 phosphorylation at Tyr^{656} [a YXXM motif (*21*), a known consensus binding site for the SH2 domains of p85].

The IFNAR1 chain undergoes IFN-dependent tyrosine phosphorylation, and several tyrosine-phosphorylated proteins coprecipitate with the IFNAR1 chain (*6, 22*). To determine whether p85 interacts with IFNAR1, we precipitated proteins from lysates of control and IFN-treated Daudi cells with an IFNAR1-specific antibody and analyzed them by blotting with antiserum to p85 (Fig. 1A). Although similar amounts of IFNAR1 chain were immunoprecipitated from treated or untreated cells (*23*), only precipitates from IFN-α–treated cells contained p85. Maximal association was observed at 5 min after IFN addition and decreased rapidly thereafter. IFNAR1 and STAT3 also coprecipitated with p85 in lysates from IFN-α–treated cells (Fig. 1B).

These results led us to investigate whether the tyrosine-phosphorylated IFNAR1 chain bound p85. The phosphorylation of conserved motifs present in the IFNAR1 subunit may create sites for high-affinity interactions with cytoplasmic proteins containing SH2 and phosphotyrosine binding (PTB) domains (*17, 18, 24, 25*). STAT3 directly binds to the tyrosine-phosphorylated IFNAR1 chain through its SH2 domain (*22*); thus, the IFNAR1 chain might also interact with the SH2 domains of p85. We prepared glutathione-S-transferase (GST) fusion proteins that encompassed the NH_2-terminal (Np85), COOH-terminal (Cp85), or both SH2 domains of p85 (N+Cp85). Lysates from IFN-α–treated Daudi cells were incubated with GST fusion proteins bound to glutathione-agarose beads. The precipitated material was analyzed by blotting with anti-IFNAR1. The fusion protein containing both SH2 domains of p85 precipitated much greater amounts than did fusion proteins containing only one SH2 domain (Fig. 2). The N+Cp85 fusion protein did not precipitate IFNAR1 from lysates from control cells or cells pretreated with the tyrosine kinase inhibitor genistein, which demonstrated that tyrosine phosphorylation is required for interaction of IFNAR1 with p85 fusion proteins. IFNAR1 did not interact with GST protein alone (*22*). N+Cp85 also precipitated tyrosine-phosphorylated STAT3 from lysates prepared from IFN-α–treated cells.

These results led us to determine whether STAT3 or IFNAR1 could directly interact with p85, as measured by direct blotting with the N+Cp85 fusion protein. Although N+Cp85 did not directly bind to tyrosine-phosphorylated IFNAR1, it did bind to tyrosine-phosphorylated STAT3 (Fig. 2C). These results suggest that a strong interaction of p85 with IFNAR1 requires both SH2 domains of p85 and that such an interaction is indirect because p85 binds directly to STAT3 but not IFNAR1. However, additional adapt-

Department of Pathology, University of Tennessee Health Science Center, Memphis, TN 38163, USA.

*These authors contributed equally to this work.
†To whom correspondence should be addressed.